T-AS/38/12//38948

Bispectral Analysis of Two-Dimensional Random Processes

Vinod Chandran
Steve Elgar

Reprinted from
IEEE TRANSACTIONS ON ACOUSTICS, SPEECH, AND SIGNAL PROCESSING
Vol. 38, No. 12, December 1990

Bispectral Analysis of Two-Dimensional Random Processes

VINOD CHANDRAN AND STEVE ELGAR

Abstract—**The techniques used for bispectrum estimation of harmonic one-dimensional random processes are extended to two-dimensional processes. Bispectral analysis of two-dimensional processes may be used to obtain information not available in one dimension, such as the detection of coupling between waves traveling in different directions. Such coupling is detectable in a noisy environment by the bispectral techniques presented here. Symmetry relations are used to reduce the size of the region of bispectral computations, but unlike the one-dimensional case, accounting for the directions of the interacting waves influences the procedure for determining the minimum required region of computation. Even with a reduced region of computation, bispectrum estimation in two dimensions is both memory and computation intensive. Bispectral analysis of numerically simulated realizations of multidimensional wave data demonstrate a) detection of nonlinear coupling between waves traveling in different directions, b) estimation of the degree of coupling of such an interaction, and c) the effect of leakage of power into sidelobes on bicoherence values both with and without windowing of the data.**

I. Introduction

In the present study, one-dimensional (1-D) bispectral techniques [1]–[6] are extended to two-dimensional (2-D) processes,

Manuscript received May 14, 1989; revised November 17, 1989. This research was supported by the Coastal Sciences Branch of the Office of Naval Research.

The authors are with the Electrical and Computer Engineering Department, Washington State University, Pullman, WA 99164-2752.

IEEE Log Number 9038948.

allowing the question of phase coupling between waves traveling in different directions to be directly addressed. Formal definitions of the 2-D bispectrum are presented in Section II. Although extending bispectral calculations to two-dimensional processes is conceptually straightforward, the technical details are nontrivial, as described in Section III. Bispectral analysis of several numerically simulated two-dimensional random processes is presented in Section IV, followed by conclusions in Section V.

II. Bispectrum in Two Dimensions

The bispectrum $B(f_{x1}, f_{y1}, f_{x2}, f_{y2})$ of a stationary, real-valued, two-dimensional random process $g(x, y)$ is defined as the Fourier transform of the third moment function $S(\tau_{x1}, \tau_{y1}, \tau_{x2}, \tau_{y2})$:

$$B(f_{x1}, f_{y1}, f_{x2}, f_{y2}) = \int_{-\infty}^{\infty}\int_{-\infty}^{\infty}\int_{-\infty}^{\infty}\int_{-\infty}^{\infty} d\tau_{x1}\, d\tau_{y1}\, d\tau_{x2}\, d\tau_{y2}\, S(\tau_{x1}, \tau_{y1}, \tau_{x2}, \tau_{y2}) \cdot \exp\left[-j2\pi(f_{x1}\tau_{x1} + f_{y1}\tau_{y1} + f_{x2}\tau_{x2} + f_{y2}\tau_{y2})\right] \quad (1)$$

where f and τ are the spatial frequencies and lags, respectively, and $S(\tau_{x1}, \tau_{y1}, \tau_{x2}, \tau_{y2}) = E[g(x, y)\, g(x + \tau_{x1}, y + \tau_{y1})\, g(x + \tau_{x2}, y + \tau_{y2})]$. $E[\cdot]$ is the expectation operator, and in practice often implies ensemble averaging. An alternative expression for the 2-D bispectrum that eliminates the need of computing the multidimensional integral is developed below similar to the 1-D case [1]–[4]. The power spectrum (which is the Fourier transform of the autocorrelation function $R(\tau_x, \tau_y) = E[g(x, y)\, g(x + \tau_x, y + \tau_y)]$) and the bispectrum are members of a class of higher order spectra for stationary random processes that are based on cumulants. The nth order cumulant function is given by $C_n(\tau_1, \tau_2, \cdots, \tau_{n-1})$

$$C_n(\tau_1, \tau_2, \cdots, \tau_{n-1}) = C[x(t)x(t + \tau_1) \cdots x(t + \tau_{n-1})] \quad (2)$$

where C stands for the cumulant average [3]–[6]. The Fourier transform of the nth order cumulant function of the random process is called its nth order cumulant spectrum [3], [4], $F_n(f_1, f_2, \cdots, f_{n-1})$. The cumulant function vanishes for time differences greater than the coherence time, thus ensuring absolute integrability, and hence the existence of the cumulant spectrum. The coherence time τ_c is defined as the time interval such that $x(t + \tau)$ can be regarded as independent of $x(t)$ when $\tau \geq \tau_c$. For functions of spatial variables an analogous coherence length may be defined. For a zero-mean, stationary random process $g(x, y)$

$$C[g(x, y)\, g(x + \tau_{x1}, y + \tau_{y1})] = E[g(x, y)\, g(x + \tau_{x1}, y + \tau_{y1})] = R(\tau_{x1}, \tau_{y1}) \quad (3)$$

and

$$C[g(x, y)\, g(x + \tau_{x1}, y + \tau_{y1})\, g(x + \tau_{x2}, y + \tau_{y2})] = E[g(x, y)\, g(x + \tau_{x1}, y + \tau_{y1})\, g(x + \tau_{x2}, y + \tau_{y2})] = S(\tau_{x1}, \tau_{y1}, \tau_{x2}, \tau_{y2}). \quad (4)$$

From equations (3) and (4) it can be observed that the power spectrum and the bispectrum are the second- and third-order cumulant spectra [2], [3], respectively, of the random process.

The cumulant spectrum for a one-dimensional process $x(t)$ may be estimated in terms of the cumulant average of the Fourier coefficients whose sum frequency vanishes, provided the record length $T \gg \tau_c$, [5]

$$F_n(f_1, f_2, \cdots, f_{n-1})\delta\left(\sum_{l=1}^{n} f_l\right) = C[X(f_1)X(f_2) \cdots X(f_n)] \quad (5)$$

where

$$\delta(f) = \begin{cases} 1 & \text{if } f = 0 \\ 0 & \text{otherwise} \end{cases}$$

and

$$X(f_k) = \lim_{T\to\infty} \frac{1}{T}\int_{-T/2}^{T/2} dt\, x(t) \exp\left[-j2\pi f_k t\right].$$

$X(f_k)$ are the Fourier coefficients for $k = 1, 2, \cdots, n$. Note that owing to the stationarity of $x(t)$, the cumulant average of the Fourier coefficients will be nonzero only when the sum frequency is zero, and thus with $f_n = -\sum_{i=1}^{n-1} f_i$ equation (5) is compatible with the definition of the nth order cumulant spectrum as a function of $n - 1$ frequencies.

Invoking the separability of the 2-D Fourier transform into a one-dimensional Fourier transform with respect to one independent variable followed by another one-dimensional transform of the result with respect to the other independent variable, (5) can be extended to 2-D random processes, yielding

$$C[G(f_{x1}, f_{y1})G(f_{x2}, f_{y2}) \cdots G(f_{xn}, f_{yn})] = F_n(f_{x1}, f_{y1}, \cdots, f_{xn-1}, f_{yn-1})\delta\left(\sum_{l=1}^{n} f_{xl}\right)\delta\left(\sum_{l=1}^{n} f_{yl}\right). \quad (6)$$

This equation suggests that the cumulant spectrum for a 2-D random process may be estimated in terms of the cumulant average of the product of the Fourier coefficients $G(f_x, f_y)$, whose sum frequency is zero in the x and y components separately. Since the Fourier coefficients are zero mean

$$C[G(f_{x1}, f_{y1})G(f_{x2}, f_{y2})G(f_{x3}, f_{y3})] = E[G(f_{x1}, f_{y1})G(f_{x2}, f_{y2})G(f_{x3}, f_{y3})]. \quad (7)$$

From (6) and (7), the bispectrum, defined as the third-order cumulant spectrum, is

$$B(f_{x1}, f_{y1}, f_{x2}, f_{y2}) = F_3(f_{x1}, f_{y1}, f_{x2}, f_{y2}) = E[G(f_{x1}, f_{y1})G(f_{x2}, f_{y2})G^*(f_{x3}, f_{y3})] \quad (8)$$

where $f_{x1} + f_{x2} = f_{x3}$ and $f_{y1} + f_{y2} = f_{y3}$. The Fourier coefficients are easily computed using a two-dimensional FFT routine. For 2-D random processes, the bispectrum is a function of 4 spatial frequency components and the triads of Fourier components are such that the component of the triad at the "sum" frequency is in the direction of the vector sum of the two "lower" frequencies. These are the same conditions on the frequencies that would be satisfied by two waves traveling in the directions represented by spatial frequencies (f_{x1}, f_{y1}) and (f_{x2}, f_{y2}) interacting nonlinearly to produce a third wave traveling in a direction represented by spatial frequency (f_{x3}, f_{y3}). The bispectrum is zero for all triads of Fourier components that do not satisfy this condition, as evident from (6), provided the signal consists only of harmonics with random phases.

III. Digital Computation of the 2-D Bispectrum

Two main approaches have been used to estimate the bispectrum of one-dimensional processes given a finite set of measurements. The parametric approach which is based on autoregressive (AR), moving average (MA) or ARMA models, provides higher resolution estimates, and may be suitable for short data records. The conventional ("Fourier type") approach is easy to implement and appropriate when there are sufficient data. An extensive list of references for each approach may be found in [6]. Two-dimensional bispectral analysis has been employed for shift-invariant imaging of photon-limited data [7]. The parametric approach for detection of nonlinear phase coupling [8] and phase reconstruction [9]–[11] has been discussed earlier, as have nonparametric models for phase reconstruction of multidimensional processes [10]. The direct "Fourier type" estimation of the bispectrum of a two-dimensional process shall be considered here with the emphasis on identifying the "nonredundant" region of computation and performing numerical simulations to demonstrate the usefulness of 2-D bispectral techniques in detecting and quantifying 2-D quadratic wave coupling.

A. Computational Procedures

Let $g_i(m, n)$, where $-M/2 \le m, n \le (M/2 - 1)$ and $i = 1, 2, \cdots, K$ be K realizations of a two-dimensional, zero-mean, stationary, ergodic (at least to third order) process. The realizations may be obtained from different spatial locations at the same instant of time or from the same spatial locations at different times. Let these 2-D data sets or images be Fourier transformed using a two-dimensional FFT routine to yield the DFT coefficients

$$G_i(f_m, f_n) = \frac{1}{M^2} \sum_{m=-M/2}^{M/2-1} \sum_{n=-M/2}^{M/2-1} g_i(m, n) \cdot \exp\left[-j2\pi(mf_m + nf_n)/M\right] \quad (9)$$

for $-M/2 \le f_m, f_n \le (M/2 - 1)$. Analogous to the 1-D case [1]–[6], the unnormalized bispectral estimate for the data is the ensemble average over the K realizations of the triple product of Fourier coefficients given by

$$B_{un}(f_{m1}, f_{n1}, f_{m2}, f_{n2}) = \frac{1}{K} \sum_{i=1}^{K} G_i(f_{m1}, f_{n1}) G_i(f_{m2}, f_{n2}) G_i^*(f_{m3}, f_{n3}) \quad (10)$$

where $f_{m3} = f_{m1} + f_{m2}$, $f_{n3} = f_{n1} + f_{n2}$ and $-M/2 \le f_{m1}, f_{m2}, f_{m3}, f_{n1}, f_{n2}, f_{n3} \le (M/2 - 1)$. In practice it is desirable to normalize this estimate to remove the dependence on the power at the component frequency pairs [5], [6]. A normalized estimate of the bispectrum may be defined as

$$B(f_{m1}, f_{n1}, f_{m2}, f_{n2}) = \frac{B_{un}(f_{m1}, f_{n1}, f_{m2}, f_{n2})}{\sqrt{\left[\frac{1}{K}\sum_{i=1}^{K} \left|G_i(f_{m1}, f_{n1}) G_i(f_{m2}, f_{n2})\right|^2\right]\left[\frac{1}{K}\sum_{i=1}^{K} \left|G_i(f_{m3}, f_{n3})\right|^2\right]}}. \quad (11)$$

Using the Cauchy–Schwarz inequality [5], it can be shown that $0 < |B| < 1$. The bispectrum is in general a complex quantity with magnitude b (bicoherence) and phase ϕ_b (biphase). For the detection of quadratic phase coupling, the bicoherence, which provides a measure of the strength of the coupling [2], [5] may be preferable to the unnormalized bispectrum.

The computation of the 2-D bispectrum even for small data sets requires large arrays. For example, when $M = 32$, without a reduction in the region of computation, the size of the bispectrum array would be 32^4, which is 1 048 576 complex numbers. The size of the arrays required can be reduced by taking advantage of the symmetry properties of the 2-D bispectrum, which follow from its definition and the fact that $G(f_m, f_n) = G^*(-f_m, -f_n)$ for a real two-dimensional process $g(m, n)$. These symmetries [7], [10], [11] differ from the one-dimensional case [1]–[6] because negation of one spatial frequency component results in an unrelated mode and does not contribute to any symmetry in the bispectrum. Thus

$$B(f_{m1}, f_{n1}, f_{m2}, f_{n2}) = B^*(-f_{m1}, -f_{n1}, -f_{m2}, -f_{n2}) \quad (12)$$

$$= B(f_{m2}, f_{n2}, f_{m1}, f_{n1}) \quad (13)$$

$$= B(f_{m1}, f_{n1}, -f_{m1} - f_{m2}, -f_{n1} - f_{n2})$$

$$= B(-f_{m1} - f_{m2}, -f_{n1} - f_{n2}, f_{m2}, f_{n2}). \quad (14)$$

Equation (12) implies that the minimum region of computation lies within the region $S_1 = \{f_{m1} > 0\} \cup \{f_{m1} = 0, f_{n1} \ge 0\}$. Interchanging (f_{m1}, f_{n1}) and (f_{m2}, f_{n2}) in (12) by virtue of the symmetry in (13), the minimum region must also lie within $S_2 = \{f_{m2} > 0\} \cup \{f_{m2} = 0, f_{n2} \ge 0\}$. If the zero frequency Fourier component $G(0, 0)$ is ignored, which is customary because a wave is always in phase with itself, then these regions become $S_1 = \{f_{m1} > 0\} \cup \{f_{m1} = 0, f_{n1} \ge 1\}$, $S_2 = \{f_{m2} > 0\} \cup \{f_{m2} = 0, f_{n2} \ge 1\}$. Equation (13) implies that the minimum region of computation is contained in $S_3 = \{f_{m1} > f_{m2}\} \cup \{f_{m1} = f_{m2}, f_{n1} \ge f_{n2}\}$. Equation (14) together with the periodicity of the 2-D bispectrum in its four variables, implies that the minimum region of computation is contained in

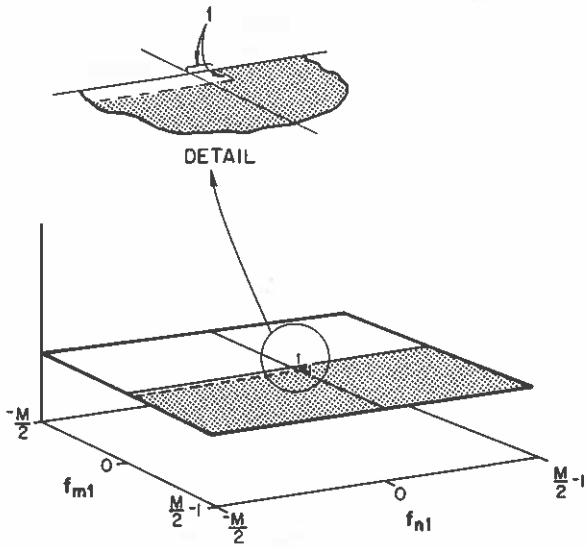

Fig. 1. Region of computation: The shaded region shows the range over which (f_{m1}, f_{n1}) is selected.

$$S_4 = \{(M/2 - 1) \ge f_{n2}, f_{n1} + f_{n2} \ge -M/2\} \cap \{(M/2 - 1) \ge f_{m2}, f_{m1} + f_{m2} \ge -M/2\}.$$

Thus the minimum region of computation is given by $S_1 \cap S_2 \cap S_3 \cap S_4$, and after some algebraic manipulation it may be specified as the intersection of these regions in the choice of f_{m1}, f_{n1}, f_{m2} and f_{n2}, yielding

$$M/2 - 1 \ge f_{m1} \ge 0 \quad (15)$$

$$M/2 - 1 \ge f_{n1} \ge \begin{cases} 1 & \text{if } f_{m1} = 0 \\ -M/2 & \text{otherwise} \end{cases} \quad (16)$$

$$\min(M/2 - f_{m1}, f_{m1}) \ge f_{m2} \ge 0 \quad (17)$$

and

$$f_{n2}^{\max} \ge f_{n2} \ge f_{n2}^{\min} \quad (18)$$

where

$$f_{n2}^{\min} = \begin{cases} 1 & \text{if } f_{m2} = 0 \\ \max(-M/2, -M/2 - f_{n1}) & \text{otherwise} \end{cases}$$

and

$$f_{n2}^{\max} = \begin{cases} \min(M/2 - 1, f_{n1}, M/2 - 1 - f_{n1}) & \text{if } f_{m1} = f_{m2} \\ \min(M/2 - 1, M/2 - 1 - f_{n1}) & \text{otherwise.} \end{cases}$$

Figs. 1 and 2 illustrate the reduced region of computation obtained by taking the symmetry properties into account. The number of 4-tuples for which the bispectrum is computed for $M = 32$ is reduced to 45 832. Every triad of Fourier components that satisfies the conditions for a sum or difference interaction will be considered as a unique sum interaction in the region of computation. For example, if two waves $(f_{x1} = 8, f_{y1} = 0)$, and $(f_{x2} = 0, f_{y2} = 8)$ undergo both sum and difference interactions, the sum interaction

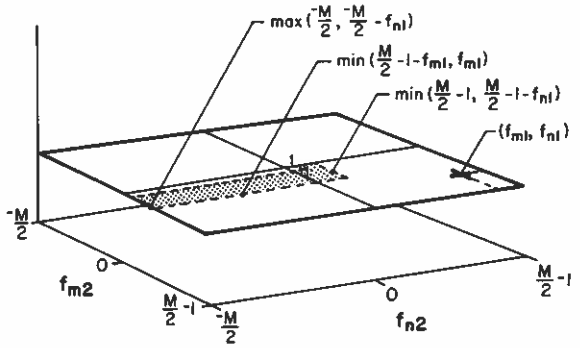

Fig. 2. Region of computation: The shaded region is the range over which (f_{m2}, f_{n2}) varies for the (f_{m1}, f_{n1}) shown (indicated by $\times$).

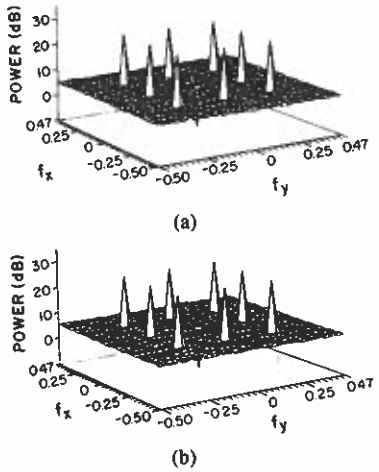

Fig. 3. Power spectra for the numerical simulations of test 1. Each spectrum is the ensemble average of 256 realizations (512 degrees of freedom). The units of power are arbitrary and the frequencies are normalized by the sampling frequency. Multiplication by $N(=32)$ yields the frequencies referred to in the text and entered in the tables. (a) Test 1a. (b) Test 1b.

will be accounted for in the triad $(f_{x1} = 8, f_{y1} = 0)$, $(f_{x2} = 0, f_{y2} = 8)$, $(f_{x3} = 8, f_{y3} = 8)$ and the difference interaction will be accounted as a "sum" interaction in the triad $(f_{x1} = 8, f_{y1} = -8)$, $(f_{x2} = 0, f_{y2} = 8)$, $(f_{x3} = 8, f_{y3} = 0)$.

IV. Tests Using Numerically Simulated Wave Data

To demonstrate the ability of the bispectrum to detect phase coupling between waves traveling in different directions, bispectral analysis was performed on numerically generated two-dimensional random processes. Each simulation generated a 32×32 realization of integer values between 0 and 255. The use of 8-b input data here is merely for economy in storage; floating point data may be used to achieve the desired numerical accuracy. Bispectra from up to 256 such images were averaged to improve the statistical confidence of the bispectral estimates. Several test cases were investigated.

A. Test 1

Test 1a consisted of waves of equal amplitude in the directions specified by the spatial frequencies $(f_x = 8, f_y = 0)$, $(f_x = 0, f_y = 8)$, $(f_x = 8, f_y = 8)$ and $(f_x = 8, f_y = -8)$, respectively. The phase of each wave was random and uniformly distributed in the interval $[0, 2\pi)$ and, thus, the waves were independent of each other. White Gaussian noise with power spectral density two orders of magnitude less than the signal power spectral densities was added to each of 256 numerically simulated realizations of the process, as shown in Fig. 3(a).

The wave field for test 1b was similar to that of test 1a, with equal amplitude waves at the same spatial frequencies as those defined for test 1a, within a background of Gaussian noise. However, for this test, the waves at $(f_x = 8, f_y = 0)$ and $(f_x = 0, f_y = 8)$ (the component waves) had random phases while those at $(f_x = 8, f_y = 8)$ and $(f_x = 8, f_y = -8)$ had phases equal to the sum of the phases of the component waves (sum interaction) and the difference of the phases of the component waves (difference interaction), respectively. The corresponding power spectral density is shown in Fig. 3(b) and it is identical to that for test 1a (Fig. 3(a)). Note that it is not possible to detect differences between the two processes (1a and 1b) from the power spectral densities.

The bicoherence values for a Gaussian process are χ^2 distributed [2] and for 256 realizations the 95% significance level for zero bicoherence is 0.108. For test 1a, 93.9% of the bicoherence values were below the theoretical 95% significance level. It is expected that approximately 5% of the values will be above 0.108, but the probability of a very high value, say greater than 0.95, occurring by random chance is extremely small [12] and values that high would have suggested phase coupling. There were no such high bicoherences for test 1a.

For the phase coupled case, the two bicoherence values corresponding to the phase-coupled triads (Table I) were greater than 0.95. Note (Table I) that the biphase values are close to zero for these triads. In this case, 94.2% of the bicoherences were below the theoretical 95% significance level for zero bicoherence. It must be pointed out here that the difference in the percentage of bicoherence values that are less than the 95% significance level for a Gaussian process between test 1b (94.2%) and test 1a (93.9%) is indeed too small to conclude that the wavefield for test 1b was non-Gaussian. In fact, although 5% of the triads may be expected to have bicoherence values greater than the 95% significance level (0.108), the probability that they have a value several standard deviations in excess of this level is very low [12] and it is this large difference between the observed bicoherence (0.991) and 95% significance level (0.108) that indicates phase coupling at that particular triad.

TABLE I
Highest Bicoherence Values for Test 1b

f_{x1}	f_{y1}	f_{x2}	f_{y2}	f_{x3}	f_{y3}	BICOHERENCE	BIPHASE
8	0	0	8	8	8	0.991	-0.18″
8	-8	0	8	8	0	0.991	-0.33″

Test 1b demonstrates that bispectral analysis of two-dimensional realizations can be used to detect quadratic nonlinear coupling of waves traveling in different directions.

B. Test 2

The purpose of this test was to demonstrate the effect of the presence of random components in addition to phase coupled ones on the bicoherence values. The three parts of this test (2a–2c) each consisted of four waves defined in the y direction having frequencies $(f_x = 0, f_y = 2)$, $(f_x = 0, f_y = 8)$, $(f_x = 0, f_y = 6)$ and $(f_x = 0, f_y = 10)$. In addition, for 2a all the waves had random phases and equal amplitudes. For 2b the first two waves had equal magnitude, while the other two (the difference and the sum interaction products) had a 25% random phase component and a 75% coupled phase component. Thus, 75% of the power at these frequencies was owing to nonlinear coupling with the first two waves, and therefore the bicoherence at the quadruples corresponding to these interactions is expected to be $\sqrt{0.75}$ (0.866). Test 2c was similar to 2b except that 50% of the power at the sum and difference frequencies was independent (i.e., random phase) and therefore the bicoherence at the quadruples corresponding to these interactions

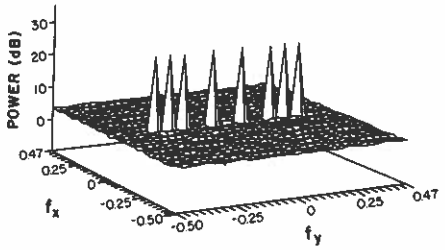

Fig. 4. Power spectrum for the numerical simulations of test 2. It is the ensemble average of 256 realizations (512 degrees of freedom). The units of power are arbitrary and the frequencies are normalized by the sampling frequency. Multiplication by $N(=32)$ yields the frequencies referred to in the text and entered in the tables.

is expected to be $\sqrt{0.5}$ (0.707). White Gaussian noise, with power two orders of magnitude less than that of the waves, was added to the realizations. The power spectrum for the three cases is shown in Fig. 4.

The results of bispectral analysis for tests 2b and 2c are listed in Tables II and III, respectively. For 2a there were no high bicoherence values. For 2b and 2c there were high bicoherence values at the quadruples that satisfy the vector conditions for the sum and difference interactions, and these values are close to those expected. The small amount of background noise acts to reduce the bicoherence slightly, on average.

Test 2 demonstrates the ability of 2-D bispectral analysis to estimate the fraction of power in a wave traveling in a particular direction owing to nonlinear interactions between waves in other directions. In general, several different modes may interact to contribute to the coupled power in a particular direction. The square of the bicoherence provides an estimate of the percent of power in a particular direction owing to quadratic nonlinear coupling with the other two waves of the triad under consideration.

C. Test 3

This test was conducted to briefly demonstrate the effect of leakage on the bicoherence values. If any of the interacting waves has a frequency that corresponds to a nonintegral number of wavelengths in the record lengths along the x or y directions, there will be leakage of power into other frequencies (resulting in sidelobes). Since the leakage power decays (rolls off) as the frequencies become farther from the true peaks, so do the bicoherence values. Data windows reduce the bispectral leakage, analogous to the reduction of leakage in the power spectrum, as demonstrated in tests 3a and 3b. The two-dimensional random process realizations in both cases consisted of waves of equal amplitude in the directions specified by the spatial frequencies ($f_x = 8.5, f_y = 0$), ($f_x = 0, f_y = 8.5$) and ($f_x = 8.5, f_y = 8.5$). The phases of the first two waves were random and uniformly distributed in the interval $[0, 2\pi)$ while the phase of the third wave was equal to the sum of the phases of the other two for each realization. For 3a no window was applied to the simulated records, while for 3b a Hamming window in two dimensions was used. Tables IV and V show the four highest bicoherences for 3a and 3b, respectively. Note that these correspond to the true frequencies within the limits of resolution set by the record length. In both cases, the power at the sidelobe frequencies is also phase coupled, resulting in high bicoherences, as shown in Fig. 5. For 3b, the Hamming window causes a sharper roll off in the bicoherence values, similar to its effect on the power spectrum (compare Fig. 5(b) and 5(a)). Note that the window itself may be considered as a superposition of waves or Fourier components and owing to the time-domain multiplication, these components will form phase-coupled triads with Fourier components present in the input. Therefore, the mean value must be removed from the input before windowing. This test demonstrates the use of a data window in reducing bicoherence leakage in two-dimensional bispectral analysis.

TABLE II
HIGHEST BICOHERENCE VALUES FOR TEST 2b

f_{x1}	f_{y1}	f_{x2}	f_{y2}	f_{x3}	f_{y3}	BICOHERENCE	BIPHASE
0	8	0	2	0	10	0.819	+3.25°
0	6	0	2	0	8	0.853	+2.78°

TABLE III
HIGHEST BICOHERENCE VALUES FOR TEST 2c

f_{x1}	f_{y1}	f_{x2}	f_{y2}	f_{x3}	f_{y3}	BICOHERENCE	BIPHASE
0	8	0	2	0	10	0.581	-5.49°
0	6	0	2	0	8	0.634	-0.76°

TABLE IV
HIGHEST BICOHERENCE VALUES FOR TEST 3a

f_{x1}	f_{y1}	f_{x2}	f_{y2}	f_{x3}	f_{y3}	BICOHERENCE	BIPHASE
9	0	0	9	9	9	0.975	-0.77°
9	0	0	8	9	8	0.974	-0.46°
8	0	0	9	8	9	0.973	+0.33°
8	0	0	8	8	8	0.974	+0.46°

TABLE V
HIGHEST BICOHERENCE VALUES FOR TEST 3b

f_{x1}	f_{y1}	f_{x2}	f_{y2}	f_{x3}	f_{y3}	BICOHERENCE	BIPHASE
9	0	0	9	9	9	0.979	-0.62°
9	0	0	8	9	8	0.979	-0.30°
8	0	0	9	8	9	0.977	-0.16°
8	0	0	8	8	8	0.980	-0.10°

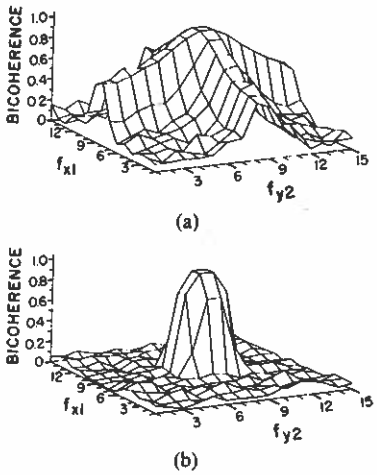

Fig. 5. A subset of all possible bicoherence values consisting of the frequency quadruples (f_{x1}, 0, 0, f_{y2}) for the numerical simulations of test 3. For $f_{x2} = 0, f_{y1} = 0$, the region of computation is $1 \le f_{x1}, f_{y2} \le (M/2 - 1)$ as discussed in the text. The interacting waves had frequency vectors ($f_{x1} = 8.5, f_{y1} = 0$) and ($f_{x2} = 0, f_{y2} = 8.5$). (a) No window, (b) Hamming window. Note the faster roll off of bicoherence in (b).

V. Conclusions

This correspondence presents the extension of bispectral analysis from one-dimensional random processes (e.g., time series) to two-dimensional random processes. Use of the symmetry properties of the bispectrum reduces the number of computations considerably. Numerical simulations demonstrate the ability of 2-D bispectral estimation to detect quadratic phase coupling between waves traveling in different directions. By windowing the data, bicoherence leakage can be reduced.

References

[1] K. Hasselmann, W. H. Munk, and G. J. F. MacDonald, "Bispectra of ocean waves," in *Time Series Analysis*, M. Rosenblatt, Ed. New York: Wiley, 1963, pp. 125–139.

[2] R. A. Haubrich, "Earth noise, 5 to 500 millicycles per second," *J. Geophys. Res.*, vol. 70, pp. 1415–1427, 1965.

[3] D. R. Brillinger and M. Rosenblatt, "Asymptotic theory of estimates of kth order spectra," in *Spectral Analysis of Time Series*, B. Harris, Ed. New York: Wiley, 1967, pp. 153–188.

[4] D. R. Brillinger and M. Rosenblatt, "Computation and interpretation of kth order spectra," in *Spectral Analysis of Time Series*, B. Harris, Ed. New York: Wiley, 1967, pp. 189–232.

[5] Y. C. Kim and E. J. Powers, "Digital bispectral analysis and its applications to nonlinear wave interactions," *IEEE Trans. Plasma Sci.*, vol. PS-7, pp. 120–131, 1979.

[6] C. L. Nikias and M. R. Raghuveer, "Bispectrum estimation: A digital signal processing framework," *Proc. IEEE*, vol. 75, pp. 869–889, 1987.

[7] H. Bartelt and B. Wirnitzer, "Shift-invariant imaging of photon-limited data using bispectral analysis," *Opt. Commun.*, vol. 53, pp. 13–16, 1985.

[8] M. R. Raghuveer and S. A. Dianat, "Detection of nonlinear phase coupling in multidimensional stochastic processes," in *Int. Conf. Adv. Contr., Commun.*, Oct. 1988, pp. 729–732.

[9] S. A. Dianat, M. R. Raghuveer, and G. Sundaramoorthy, "Reconstruction of nonminimum phase multidimensional signal using the bispectrum," in *SPIE Conf. Visual Commun., Image Processing III*, Nov. 1988, pp. 666–671.

[10] A. Swami and G. B. Giannakis, "ARMA modeling and phase reconstruction of multidimensional non-Gaussian processes using cumulants," in *Proc. ICASSP-88* (New York, NY), Apr. 1988, pp. 729–732.

[11] S. A. Dianat and M. R. Raghuveer, "Two-dimensional nonminimum phase signal reconstruction," in *Proc. Workshop Higher Order Spectral Anal.* (Vail, CO), June 1989, pp. 666–671.

[12] S. Elgar and G. Sebert, "Statistics of bicoherence and biphase," *J. Geophys. Res.*, vol. 94, 1989, pp. 10993–10998.